

# Binding Energies of Hydrogen-Bonded *cis*-Amide and Nucleobase Dimers: An Evaluation of DFT Performance

Jann A. Frey and Samuel Leutwyler\*

**Abstract:** The understanding of biological processes at the molecular level demands accurate knowledge of the nonbonded interactions that control the geometries, binding energies and dynamics of the supramolecular structures involved. High level *ab initio* methods are still prohibitively expensive for large systems, but certain density functional (DFT) methods can provide cost-effective alternatives. The performance of six different functionals (BLYP, B3LYP, X3LYP, PBE, PW91, and mPW91) for the calculation of the doubly hydrogen-bonded *cis*-amide dimers (formamide)<sub>2</sub> and (2-pyridone)<sub>2</sub> have been tested. Their N-H...O hydrogen bond motifs occur between many nucleobases, peptides, and proteins. Binding energy benchmarks using *ab initio* MP2 calculations and basis set extrapolations to the complete basis set (CBS) limit with the Dunning aug-cc-pVXZ (X=D,T,Q) basis set series have been established. These yield  $D_e^\infty = -14.80$  kcal/mol for (formamide)<sub>2</sub> and  $-22.63$  kcal/mol for (2PY)<sub>2</sub>. Of the six functionals, PW91 consistently gives the best agreement with the MP2 basis-set limit binding energies, closely followed by PBE. The mPW91, B3LYP and the recently proposed X3LYP functionals are in less good agreement. The BLYP functional underestimates the interaction strengths by 20–25% and is not recommended. As an application the hydrogen-bond isomerization equilibria for the Sugar-edge, Watson-Crick and Wobble isomers of the dimers 2-pyridone-uracil and 2-pyridone-thymine from first principles are computed and compared to experiment.

**Keywords:** Binding energies · Density functional · Formamide dimer · Hydrogen bonds · 2-Pyridone dimer

## 1. Introduction

The accurate computation of intermolecular interaction energies is fundamental for the prediction of structures, isomers, tautomers, and supramolecular interactions of systems of biological interest, such as polypeptides, enzymes, oligonucleotides, and nucleic acids. High-level correlated *ab initio* approaches such as CCSD(T) give very accurate structures and interaction en-

ergies but consume tremendous amounts of CPU time even for small systems and are therefore not applicable to large systems. Structure and dynamics in systems of biological interest are usually still modeled using empirical force fields [1–4]. This approach is adequate to obtain qualitative and global structural information, but the lack of accurate intermolecular potentials and intrinsic methodological restrictions of the force field approach [5] hinder more accurate investigations of structures and energies. Due to their computational efficacy, density functionals involving the generalized gradient approximation (GGA) [6–14] have become popular for the calculation of intermolecular interactions between medium-size molecules. The quality of different exchange and correlation functionals is usually judged by their predictions of the chemical binding energies of the G2 test set [15], but this set does not include intermolecular interactions. For benchmarking intermolecular interactions of larger systems, the amount of accurate experimental data is still very limited. An alternative is then to compare to high-level correlated *ab initio* calculations.

Several studies have investigated the accuracy of DFT methods for intermolecular

interactions: Tsuzuki and Lüthi [16] examined the performance of different functionals for systems from rare-gas dimers to H-bonded dimers. They employed the Dunning correlation-consistent cc-pVXZ (X = D,T,Q and 5) basis set series (without diffuse functions) and compared to second-order Møller-Plesset (MP2) and coupled cluster CCSD(T) results. Other approaches have combined DFT with dispersive correction terms in order to account for correlation effects [17–20]. Typically, dispersive atom–atom interaction terms are added to functionals that themselves do not exhibit minima for rare-gas dimers, such as BLYP and B3LYP [16]. The improvements are achieved at the price of adding a (large) number of atom–atom parameters that have to be empirically fitted [17–20]. In contrast to these supermolecule approaches, Wesolowski and co-workers have implemented a variational DFT approach for the calculation of weakly bound complexes based on the total energy bifunctional  $E[\rho_1, \rho_2]$ , the so-called Kohn-Sham procedure with constrained electron density (KSCED) [21–25]. For weakly-bound complexes the calculated geometries and binding energies are in good agreement with experiment and/or high-level calculations [21–26].

\*Correspondence: Prof. Dr. S. Leutwyler  
Universität Bern  
Departement für Chemie und Biochemie  
Freiestrasse 3  
CH-3000 Bern 9  
Tel.: +41 31 631 44 79  
Fax: +41 31 631 39 94  
E-Mail: samuel.leutwyler@iac.unibe.ch

Our group has investigated the hydrogen-bond interactions of nucleobases and nucleobase analogues, both experimentally in molecular beams and theoretically using DFT and *ab initio* methods [27–35]. The spectra of the pyrimidine nucleobases uracil (U) and thymine (T, 5-methyluracil) in supersonic jets are broad [36] due to their ultrarapid nonradiative decay [37][38]. In order to circumvent these photophysical limitations, we employ 2-pyridone (2PY), shown in Fig. 1, as a nucleobase mimic: 2PY and its self-dimer (2PY)<sub>2</sub> exhibit narrow-band absorption and emission spectra [27][28][39][40]. Like the pyrimidine nucleobases, 2PY has neighboring N–H donor and C=O acceptor groups. (2PY)<sub>2</sub> is bound by antiparallel N–H...O=C hydrogen bonds, analogous to the uracil wobble dimer U·U [41][42]. The symmetric doubly hydrogen-bonded structure [39][40], intermolecular vibrations [27] and ultrafast excited-state energy transfer [28] of (2PY)<sub>2</sub> have been studied. We have systematically investigated doubly hydrogen-bonded dimers of 2PY with U, T, 3-methyluracil (3MU), 1-methyluracil (1MU), and 5-fluorouracil (5FU) [33][35]. As shown in Fig. 1, the pyrimidine nucleobases offer three different hydrogen-bonding sites: the canonical Watson-Crick (WC), the Wobble (W) and the Sugar-edge (S). In the biological context, the N1 atom is linked to the (desoxy)ribose, so the Sugar-edge sites are not accessible for double hydrogen bonding. Accurate calculations of the binding energies of all possible dimers are needed to help determine the identity of the dimer(s) that are examined in the experiments.

We first present a comparative *ab initio* and DFT study of two model systems, (formamide)<sub>2</sub> and (2-pyridone)<sub>2</sub>, abbreviated (FA)<sub>2</sub> and (2PY)<sub>2</sub>. These doubly N–H...O hydrogen-bonded dimers serve as mimics for U·U, T·T and analogous dimers that have been crystallographically observed in RNAs and tRNAs. The electronic binding energies  $D_e$  are fundamental properties of the intermolecular interaction but are not directly measurable; one also needs accurate vibrational frequencies to obtain the experimentally accessible dimer dissociation energy  $D_0$ . At finite temperatures, both rotational constants and vibrational frequencies are needed for the calculation of the dimer thermodynamic functions such as  $\Delta_{\text{dim}}^H$ ,  $\Delta_{\text{dim}}^S$ ,  $\Delta_{\text{dim}}^G$ , and the dimerization constant  $K_{\text{dim}}$ . *Ab initio* correlated methods are still too expensive to calculate the required vibrational frequencies; we show that selected DFT methods allow the calculation of these with very good accuracy. We apply the DFT results to calculate the dimerization equilibria of three different 2PY-uracil and 2PY-thymine isomers from first principles, and compare them to experiment [35].

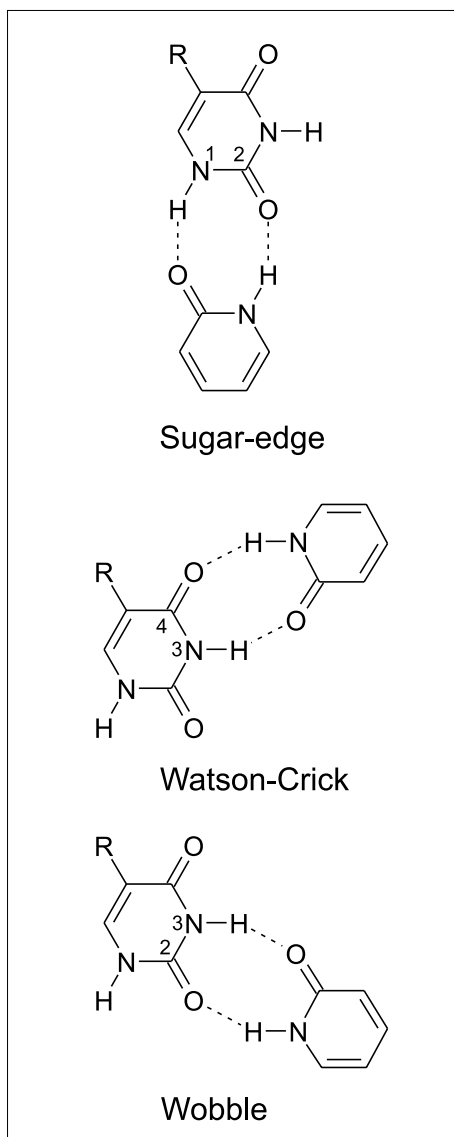


Fig. 1. Three hydrogen-bond isomers of 2-pyridone-uracil: (a) Sugar-edge (2PY·U1), (b) Watson-Crick (2PY·U2) and (c) Wobble (2PY·U3). The analogous Sugar-edge, Watson-Crick and Wobble isomers of 2-pyridone-thymine are discussed in the text and the R2PI spectra shown in Fig. 5.

## 2. Theoretical Results and Discussion

### 2.1. Theoretical Methods

Benchmark calculations of structures and binding energies were carried out with the frozen-core MP2 method: full structure optimizations of (FA)<sub>2</sub> and (2PY)<sub>2</sub> were performed with the Dunning aug-cc-pVTZ basis set, using the most stringent convergence criteria ( $<2 \times 10^{-6} E_h a_0^{-1}$ ). At these geometries, single-point calculations were performed with the aug-cc-pVXZ (X = 2, 3, 4) series of basis sets. Details of the MP2 calculations for (2PY)<sub>2</sub> have been previously given [32]. The calculations for (FA)<sub>2</sub> presented here are new: although pre-

vious MP2 calculations have been reported for (FA)<sub>2</sub> [16][45], these have employed much smaller basis sets for the structure optimizations. The basis set superposition error (BSSE) and counterpoise (CP) corrections were calculated by the Boys-Bernardi scheme [44]. Both the CP-corrected and -uncorrected binding energies  $D_e^{CP}$  and  $D_e$  were extrapolated to the complete basis set (CBS) limit,  $D_e^\infty$  by fitting the aug-cc-pVXZ (X = 2, 3, 4) binding energies to the extrapolation function proposed by Klopner [45].

DFT calculations were performed with the BLYP, B3LYP, PBEPBE, mPW91PW91, X3LYP and PW91 functionals [6–14]. With every functional, the respective geometries of the monomers and dimers were optimized with the 6-311++G(d,p) basis set (convergence criteria  $<2 \times 10^{-6} E_h a_0^{-1}$ ). The ultrafine grid was applied for numerical integration. To check the effects of basis set size we have also calculated the CBS extrapolated binding energies with the PW91 density functionals. The X3LYP calculations were performed with JAGUAR 5.0 [46], all other calculations with GAUSSIAN03 [47].

### 2.2. Benchmark Calculations on (Formamide)<sub>2</sub> and (2-Pyridone)<sub>2</sub>

The CP-corrected and -uncorrected MP2 binding energies  $D_e^{CP}$  and  $D_e$  of (FA)<sub>2</sub> and (2PY)<sub>2</sub> are given in Table 1. As shown in Fig. 2, they approach the CBS limit nearly symmetrically from above and below as a function of basis set size. For both (FA)<sub>2</sub> and (2PY)<sub>2</sub> the averages of  $D_e^{CP}$  and  $D_e$  (marked x in Fig. 2) provide very good estimates for the CBS limit values. The CBS extrapolation procedure yields binding energies  $D_{e,CBS} = -14.86$  kcal/mol and  $D_{e,CBS}^{CP} = -14.72$  kcal/mol for (FA)<sub>2</sub>. The CBS limit indicated in Fig. 2 is the average of these two values,  $D_e^\infty = -14.79$  kcal/mol. The CBS extrapolated binding energies for (2PY)<sub>2</sub> are  $D_{e,CBS} = -22.56$  kcal/mol and  $D_{e,CBS}^{CP} = -22.69$  kcal/mol [32]; the average, shown in Fig. 2 is  $-22.63$  kcal/mol. As usual, the BSSE effects on the MP2 binding energies are large and decrease relatively slowly with increasing basis set size. The relatively large residual BSSE of 4%, even at the largest basis set size, contributes an error to the CBS extrapolated binding energy that we estimate to be 0.1 kcal/mol or 0.4–0.7% of  $D_{e,CBS}$ .

Tsuzuki and Lüthi have previously investigated (FA)<sub>2</sub> with the cc-pVXZ (X = D,T,Q,5) basis sets, which lack diffuse orbitals [16]. They report an MP2/cc-pVXZ CBS limit binding energy of  $D_e^\infty = -13.40$  kcal/mol, which is 1.4 kcal/mol or  $\approx 10\%$  smaller than that obtained here. We note that they optimized the geometries at the MP2/6-311G(d,p) level. With this relatively small basis set we obtain hydrogen

Table 1. Calculated MP2 and PW91 binding energies of (formamide)<sub>2</sub> and (2-pyridone)<sub>2</sub> [kcal/mol], using the aug-cc-pVXZ (X= D, T, Q) basis sets. The energies were computed at the respective optimized aug-cc-pVTZ geometries.

MP2	(formamide) <sub>2</sub>		(2-pyridone) <sub>2</sub>	
	D <sub>e</sub>	D <sub>e</sub> <sup>CPC</sup>	D <sub>e</sub>	D <sub>e</sub> <sup>CPC</sup>
aug-cc-pVDZ	-15.598	-13.388	-24.735	-20.996
aug-cc-pVTZ	-15.362	-14.109	-23.854	-21.984
aug-cc-pVQZ	-15.073	-14.482	-23.240	-22.359
CBS limit <sup>a</sup>	-14.86	-14.72	-22.56	-22.69
PW91				
aug-cc-pVDZ	-15.839	-15.068	-22.642	-21.719
aug-cc-pVTZ	-14.952	-14.706	-21.340	-21.010
aug-cc-pVQZ	-14.564	-14.446	-21.119	-20.993
CBS limit <sup>a</sup>	-14.193	-14.184	-20.942	-21.008
6-311++G(d,p)	-14.966 <sup>b</sup>	-14.466 <sup>b</sup>	-21.683 <sup>b</sup>	-20.794 <sup>b</sup>

<sup>a</sup>Extrapolation to the complete basis set limit according to [44]; <sup>b</sup>computed at the 6-311++G(d,p) geometry

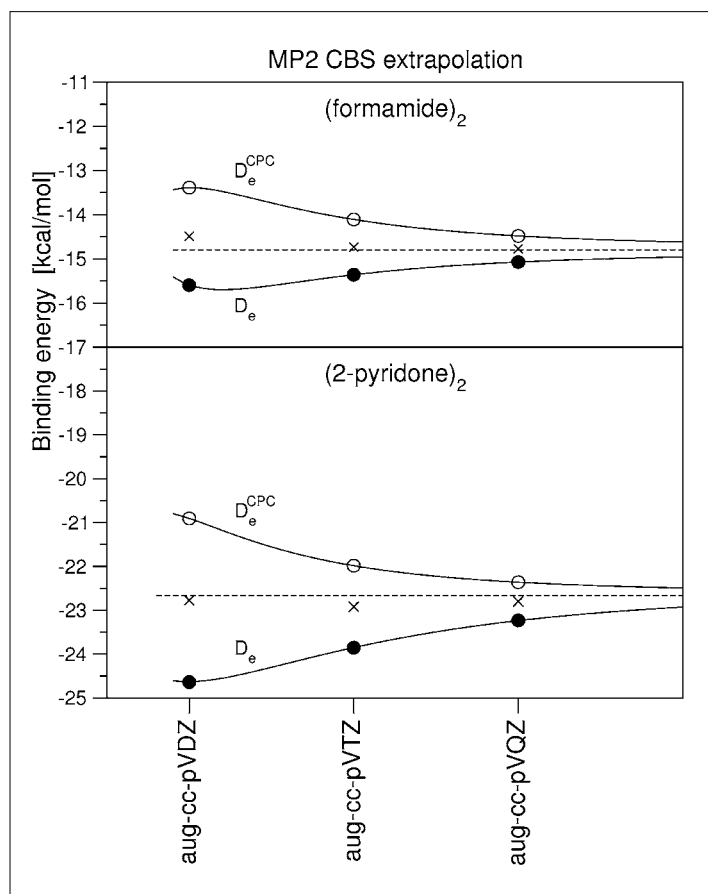


Fig. 2. MP2 calculated binding energies D<sub>e</sub> (•) and counterpoise-corrected binding energies D<sub>e</sub><sup>CPC</sup> (◦) of (formamide)<sub>2</sub> and (2-pyridone)<sub>2</sub>, using the aug-cc-pVXZ (X=D,T,Q) basis sets. Both sets of energies are extrapolated to the complete basis set (CBS) limits, as indicated by dashed lines.

bond distances of H···O = 1.897 Å (N···O = 2.914 Å), which is 0.063 Å longer than the aug-cc-pVTZ H-bond distance. Part of their smaller CBS extrapolated binding energy is thus due to the use of a nonoptimal geometry. Vargas *et al.* have performed an MP2 CBS study on five different isomers of (formamide)<sub>2</sub> with the aug-cc-pVXZ basis sets, including the C<sub>2h</sub> symmetric dimer studied here. However, there are problems with their reported results (*cf.* [48]), as becomes clear from examination of their Fig. 2 [49].

### 2.3. Comparison of the B3LYP, X3LYP and PW91 Functionals

We now employ the MP2 CBS binding energies as benchmarks for a number of density functionals that have been used to calculate intermolecular interactions: These are the GGA functionals BLYP [6][7], PW91/PW91 [10], (denoted PW91) and its modified form mPW91/PW (denoted mPW91) [13]. The PBE functional has been specifically developed for the calculation of intermolecular interactions [12]. The hybrid three-parameter functional B3LYP [11] has found widespread use due to its good chemical accuracy [14] and performance for intermolecular interactions [16]. We include the recently developed X3LYP functional of Xu and Goddard which is a combination of the B3LYP and PW91 functionals [14].

The calculated DFT binding energies for (FA)<sub>2</sub> and (2PY)<sub>2</sub> are plotted in Fig. 3. As already noted by Tsuzuki and Lüthi [16], the BLYP functional underestimates hydrogen-bond interactions by about 20–25%, and the B3LYP functional by about 15%. The mPW91 functional gives results very similar to B3LYP. In contrast, the PW91 functional yields H-bond binding energies that very close to the MP2 results, resulting in the best performance of the six functionals tested here. The PBE functional gives results that are closest to PW91 for these doubly H-bonded dimers; however, PBE has recently been criticized for its performance on chemical problems, compared to B3LYP or PW91 [50]. The X3LYP functional has been explicitly optimized for optimum performance on *both* chemical and intermolecular problems, *e.g.* the water dimer [14]. Since it is a combination of B3LYP and PW91, it is no surprise that the calculated binding energy is intermediate between those of B3LYP and PW91, hence X3LYP is inferior to PW91 on these doubly H-bonded dimers.

### 2.4. PW91 Complete Basis Set Extrapolations

Given the good performance of PW91 for the binding energies of (FA)<sub>2</sub> and (2PY)<sub>2</sub> we investigated the basis set dependence of PW91 with the aug-cc-pVXZ basis set series: The CP-corrected and -uncorrected

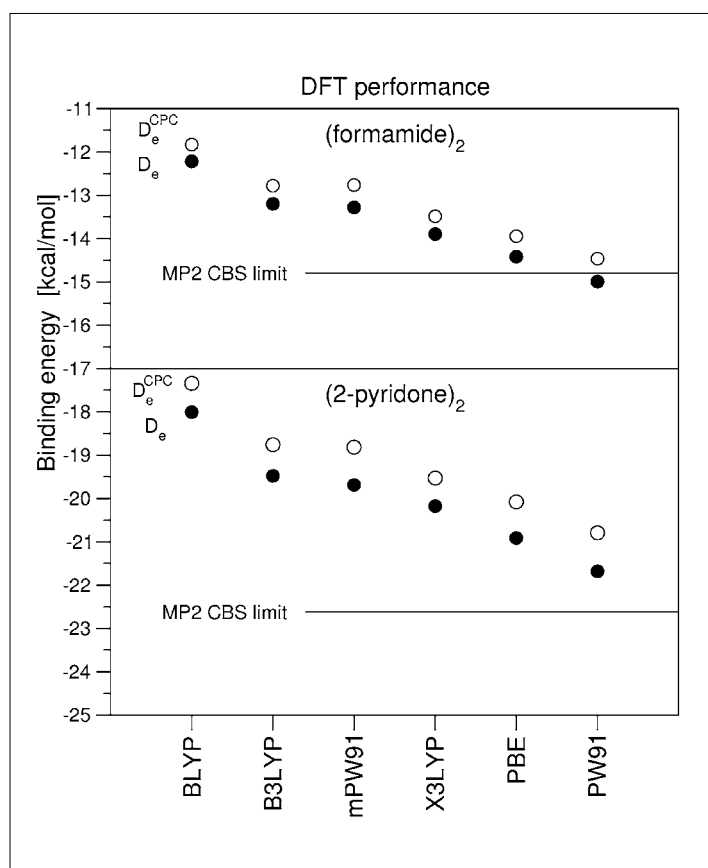


Fig. 3. Comparison of six different density functionals for the calculation of  $D_e$  (•) and counterpoise-corrected binding energies  $D_e^{CPC}$  (°) of (formamide)<sub>2</sub> and (2-pyridone)<sub>2</sub>, using the 6-311++G(d,p) basis set. The functionals are defined in the text. The MP2 complete basis set limit binding energies (formamide)<sub>2</sub> and (2-pyridone)<sub>2</sub> are given for reference. For both systems, the uncorrected PW91 binding energy  $D_e$  (•) is closest to the MP2 CBS limit.

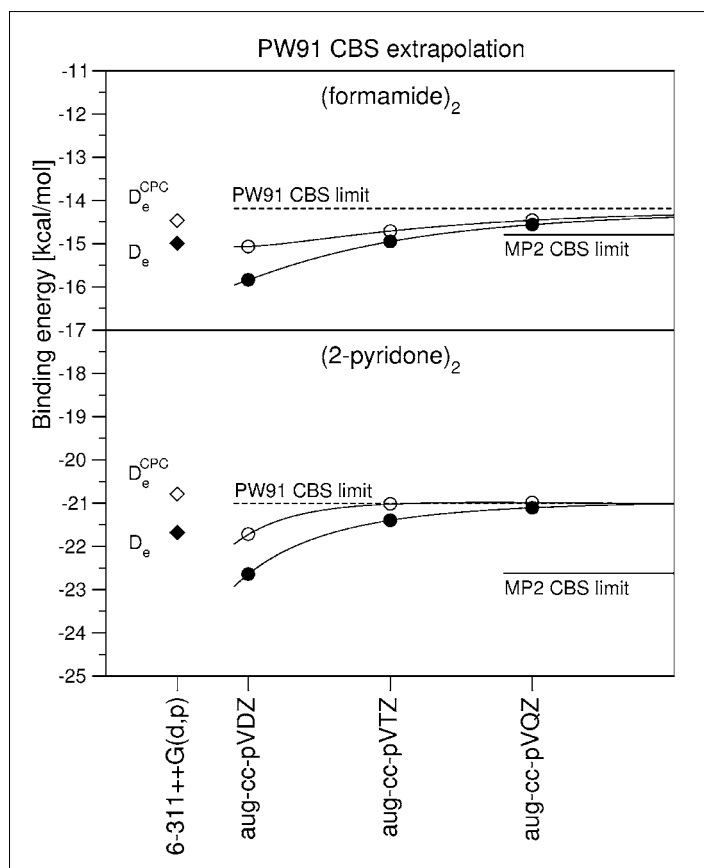


Fig. 4. Complete basis set (CBS) extrapolations of the binding energies  $D_e$  (•) and counterpoise-corrected binding energies  $D_e^{CPC}$  (°) of (formamide)<sub>2</sub> and (2-pyridone)<sub>2</sub> with the PW91 functional, using the aug-cc-pVXZ (X = D, T, Q) basis sets. The 6-311++G(d,p) binding energies are also shown on the left. The PW91 limits are given by dashed lines, the corresponding MP2 CBS limits (cf. Fig. 2) by full lines.

$D_e^{CPC}$  and  $D_e$  and the CBS binding energies  $D_{e,CBS}$  and  $D_{e,CBS}^{CPC}$  are given in Table 1. As Fig. 4 shows, the binding energies extrapolate to  $D_e = -14.19$  kcal/mol and  $-14.18$  kcal/mol for (FA)<sub>2</sub> and to  $D_{e,CBS} = -20.94$  kcal/mol and  $D_{e,CBS}^{CPC} = -21.01$  kcal/mol for (2PY)<sub>2</sub>.

The effect of basis set size on the PW91 binding energies is moderate: for (FA)<sub>2</sub> and for (2PY)<sub>2</sub> the  $D_{e,CBS}$  values are 12% and 8% smaller than the uncorrected aug-cc-pVDZ binding energies, respectively. At the CBS limit, the PW91 method underestimates by 5% for (FA)<sub>2</sub>, and by 7% for (2PY)<sub>2</sub>, relative to the MP2  $D_e^\infty$ . The calculated counterpoise corrections for PW91 are smaller than for the MP2 calculations. As a consequence, the extrapolated CP-corrected and uncorrected values lie much closer together than the MP2 values, differing by only 0.006% (0.009 kcal/mol) for (FA)<sub>2</sub> and by 0.3% (0.066 kcal/mol) for (2PY)<sub>2</sub>. In contrast to MP2, with PW91 both the CP-corrected and uncorrected binding energies approach the CBS limit from below: this implies that the counterpoise procedure underestimates the basis set incompleteness and even the CP-corrected binding energies are too large.

Fig. 4 also shows the good performance of the 6-311++G(d,p) set (378 basis functions) in comparison to the aug-cc-pVXZ basis sets, which have 412, 874 and 1580 basis functions for X = D, T and Q, respectively. For (FA)<sub>2</sub>, the uncorrected PW91 binding energy  $D_e$  approaches the MP2 extrapolated energies to within  $\approx 1.3\%$  and for (2PY)<sub>2</sub> to within  $\approx 4.2\%$  [32], giving binding energies that are comparable to those calculated with much larger basis sets. Since DFT calculations scale with the number of basis functions  $N$  as  $\approx N^{3.5}$  but MP2 as  $\approx N^5$ , this suggests the use of PW91/6-311++G(d,p) for the efficient and accurate calculation of hydrogen-bonded nucleobases.

### 2.5. Application of PW91 to Nucleobase Dimers of Uracil or Thymine with 2PY

As a practical application, we show experimental data on nucleobase dimers that involve hydrogen-bond isomerization equilibria in the gas phase. Using mass-specific resonant two-photon ionization (R2PI) spectroscopy in supersonic jets, we have measured the  $S_1 \leftarrow S_0$  vibronic spectra of the nucleobase dimers 2-pyridone-uracil

and 2-pyridone-thymine, shown in Fig. 5. The R2PI signals are composed of partially overlapping spectra due to the hydrogen-bonded isomers Sugar-edge (S), Watson-Crick (WC), and Wobble (W), shown in Fig. 1. The isomers are formed within the molecular-beam source and are in mutual equilibrium at the source temperature and pressure. Hence the reactants 2-pyridone and uracil have identical gas-phase densities for all three reactions. The same is true for the analogous dimerization reactions of 2PY with thymine, see Fig. 5(b).

To interpret the relative abundances of these isomers one needs accurate structures (*i.e.* rotational constants), intermolecular vibrational frequencies, zero-point frequencies and binding energies for all isomers. From these, the dimerization enthalpies  $\Delta_{\text{dim}}H^0$ , free energies  $\Delta_{\text{dim}}G^0$  and entropies  $\Delta_{\text{dim}}S^0$  can be calculated by gas-phase statistical mechanics [51]. The vibrational frequencies cannot be calculated by MP2 correlated *ab initio* methods, even with medium-sized basis sets, but this is possible with DFT methods. Using the PW91/6-311++G(d,p) structures, vibrational frequencies and dissociation energies of the

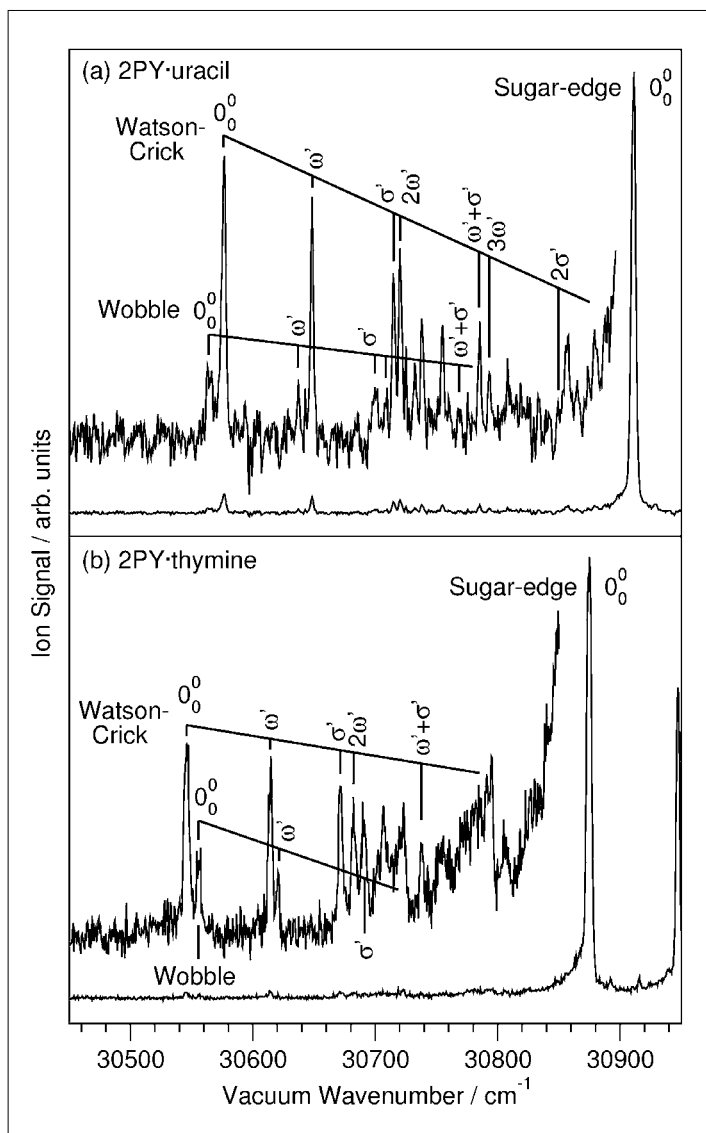


Fig. 5. Resonant two-photon ionization spectra of (a) 2-pyridone-uracil and (b) 2-pyridone-thymine. Note the weak signals between 30'500 and 30'800  $\text{cm}^{-1}$  which are due to the Watson-Crick and Wobble isomers; these signals are magnified 10 times in the inserts. The strong electronic origin bands at the right are due to the respective Sugar-edge isomers. The structures are shown in Fig. 1.

Table 2. Binding and dissociation energies  $D_e$  and  $D_0$  of the 2-pyridone-uracil and 2-pyridone-thymine Sugar-edge (U1, T1), Watson-Crick (U2, T2) and Wobble (U3, T3) isomers. The dimerization enthalpies  $\Delta_{\text{dim}}H_{298}^0$ , free energies  $\Delta_{\text{dim}}G_{298}^0$  and entropies  $\Delta_{\text{dim}}S_{298}^0$  are at room temperature, the isomerization free energies  $\Delta_{\text{isom}}G_T^0$  at the nozzle temperature  $T$ . All values calculated with the PW91 method and the 6-311++G(d,p) basis set.

	Sugar Edge		Watson-Crick		Wobble	
	U1	T1	U2	T2	U3	T3
$D_e$	-20.7	-20.5	-16.7	-16.4	-15.3	-14.8
$D_0$	-19.8	-19.6	-15.8	-15.7	-14.6	-14.8
$\Delta_{\text{dim}}H_{298}^0$	-19.6	-19.44	-15.76	-15.47	-14.26	-14.50
$\Delta_{\text{dim}}G_{298}^0$	-8.36	-8.30	-4.84	-4.56	-3.50	-3.70
$\Delta_{\text{dim}}S_{298}^0$ <sup>a</sup>	-37.6	-37.4	-36.6	-36.6	-36.1	-36.0
$\Delta_{\text{isom}}G_T^0$	0.0	0.0	3.30 <sup>b</sup>	3.59 <sup>c</sup>	4.51 <sup>b</sup>	4.37 <sup>c</sup>

<sup>a</sup>kcal/mol·K; <sup>b</sup>relative to U1 at  $T = 513$  K; <sup>c</sup>relative to T1 at  $T = 481$  K

three isomers in Table 2, we calculated the thermodynamic functions for 2PY-uracil and 2PY-thymine. From the differences of the  $\Delta_{\text{dim}}G^0$  values the equilibrium constants for the isomerization reactions Sugar-edge  $\rightarrow$  Watson-Crick and Sugar-edge  $\rightarrow$  Wobble can be obtained. For 2PY-uracil at 513 K we calculate  $\Delta_{\text{isom}}G^0 = +3.30$  kcal/mol for the Sugar-edge(U1)  $\rightarrow$  Watson-Crick(U2) and  $\Delta_{\text{isom}}G^0 = +4.51$  kcal/mol for the Sugar-edge(U1)  $\rightarrow$  Wobble(U3) isomerization, see also Table 2. These free energy changes correspond to abundances of 3.9 % for the Watson-Crick and 1.2 % for the Wobble isomer in the source at 513 K. The measured R2PI signals are  $4.2 \pm 0.25\%$  (U2) and  $1.2 \pm 0.25\%$  (U3) of the Sugar-edge (U1) electronic origin, see Fig. 5. The calculated and measured isomer ratios are seen to agree within the experimental error.

For 2PY-thymine at 481 K the calculated  $\Delta_{\text{isom}}G^0$  is +3.59 kcal/mol for the Sugar-edge Watson-Crick isomerization, see Table 2. This leads to a calculated abundance of 2.4%, in good agreement with the measured abundance of  $1.7 \pm 0.3\%$ . For the Sugar-edge(T1)  $\rightarrow$  Wobble(T3) isomerization the calculated  $\Delta_{\text{isom}}G^0$  is +4.37 kcal/mol. The predicted abundance of the Wobble isomer T3 is 1.0%, in good agreement with the measured concentration ratio of  $0.7 \pm 0.25\%$ .

### 3. Conclusions and Outlook

As a benchmark and basis for the comparisons of different density functionals, we have established MP2 complete basis set values for the binding energies of two doubly hydrogen-bonded *cis*-amide dimers, the (formamide)<sub>2</sub> dimer with  $D_e^\infty = -14.79$  kcal/mol and the (2-pyridone)<sub>2</sub> dimer with  $D_e^\infty = -22.63$  kcal/mol. The latter gas-phase dimer exhibits an extraordinarily large single N-H $\cdots$ O=C hydrogen bond energy of 11.3 kcal/mol [32].

The binding energies of the same systems are then calculated with six DFT methods that have been widely applied for the calculation of intermolecular interactions: BLYP, B3LYP, X3LYP, PBE, PW91, and mPW91. PW91 and PBE provide binding energies within a few percent of the correlated *ab initio* values, making these functionals very attractive for applications to large biochemical systems.

Compared to the very time-consuming MP2 method, the PW91 density functional can give a reliable and balanced description of hydrogen bonding in the vicinity of the minimum at a fraction of the computational cost. Although the long-range dispersive attraction forces are not correctly described by the current GGA functionals, effective error cancellation occurs at typical hydrogen bond distances. Combining PW91 with

the aug-cc-pVXZ basis sets does not improve the agreement with the MP2 values, as shown by extrapolation to the complete basis set limit. Optimum PW91 binding energies are obtained with the medium-sized 6-311++G(d,p) basis set.

The B3LYP functional and its recent offspring X3LYP, which show excellent chemical accuracies as evaluated on the G2 test [14][50], predict hydrogen bond energies in these systems that are 10–15% too small. The most commonly used GGA functional BLYP underbinds by 20–25%.

The excellent performance of PW91 is highlighted by performing a statistical-mechanics calculation of the thermodynamical functions and equilibrium constants for the gas-phase dimerization reactions of 2-pyridone with the nucleobases uracil and thymine. The calculated data is in excellent agreement with the measured ratios of the observed Sugar-edge, Watson-Crick and Wobble H-bonded isomers.

#### Acknowledgments

This work is supported by the Schweiz. Nationalfonds (Project No. 200020-105490) and via a Large User Project at the CSCS supercomputer center in Manno.

Received: June 10, 2005

- [1] T.E. Cheatham, P.A. Kollman, *Annu. Rev. Phys. Chem.* **2000**, *51*, 435.
- [2] M. Karplus, J.A. McCammon, *Nat. Struct. Biol.* **2002**, *9*, 646.
- [3] D.R. Mack, T.K. Chiu, R.E. Dickerson, *J. Mol. Bio.* **2001**, *312*, 1037.
- [4] T.A. Soares, X. Daura, C. Oostenbrink, L. J. Smith, W.F. van Gunsteren, *J. Biol. NMR* **2004**, *30*, 407.
- [5] J.K. Weltman, G. Skowron, G.B. Loriot, *J. Mol. Model.* **2004**, *10*, 367.
- [6] A.D. Becke, *Phys. Rev. A* **1988**, *38*, 3098.
- [7] C. Lee, W. Yang, R.G. Parr, *Phys. Rev. B* **1988**, *37*, 785.
- [8] J.P. Perdew, *Phys. Rev. B* **1986**, *33*, 8822.
- [9] J.P. Perdew, *Phys. Rev. B* **1986**, *34*, 7046.
- [10] J.P. Perdew, Y. Wang, *Phys. Rev. B* **1992**, *45*, 13244.
- [11] A.D. Becke, *J. Chem. Phys.* **1993**, *98*, 5648.
- [12] J.P. Perdew, K. Burke, M. Ernzerhof, *Phys. Rev. Lett.* **1996**, *77*, 3865.
- [13] C. Adamo, V. Barone, *J. Chem. Phys.* **1998**, *108*, 664.
- [14] X. Xu, W.A. Goddard, *Proc. Natl. Acad. Sci.* **2004**, *101*, 2673.
- [15] L.A. Curtiss, K. Raghavachari, G.W. Trucks, J.A. Pople, *J. Chem. Phys.* **1991**, *94*, 7221.
- [16] S. Tsuzuki, H.P. Lüthi, *J. Chem. Phys.* **2001**, *114*, 3949.
- [17] X. Wu, M.C. Vargas, S. Nayak, V. Lotrich, G. Scoles, *J. Chem. Phys.* **2001**, *115*, 8748.
- [18] Q. Wu, W. Yang, *J. Chem. Phys.* **1997**, *116*, 7921.
- [19] U. Zimmerli, M. Parrinello, P. Koumoutsakos, *J. Chem. Phys.* **2004**, *120*, 2693.
- [20] S. Grimme, *J. Comput. Chem.* **2004**, *25*, 1463.
- [21] T.A. Wesolowski, A. Warshel, *J. Phys. Chem.* **1993**, *97*, 8050.
- [22] T.A. Wesolowski, A. Warshel, *J. Phys. Chem.* **1994**, *98*, 5183.
- [23] F. Tran, J. Weber, T.A. Wesolowski, *Helv. Chim. Acta* **2001**, *84*, 1489.
- [24] T.A. Wesolowski, P.-Y. Morgantini, J. Weber, *J. Chem. Phys.* **2002**, *116*, 6411.
- [25] T.A. Wesolowski, F. Tran, *J. Chem. Phys.* **2003**, *118*, 2072.
- [26] T.A. Wesolowski, *J. Chem. Phys.* **1997**, *106*, 8516.
- [27] A. Müller, F. Talbot, S. Leutwyler, *J. Chem. Phys.* **2000**, *112*, 3717.
- [28] A. Müller, F. Talbot, S. Leutwyler, *J. Chem. Phys.* **2002**, *116*, 2836.
- [29] D.R. Borst, J.R. Roscioli, D.W. Pratt, G.M. Florio, T.S. Zwier, A. Müller, S. Leutwyler, *J. Chem. Phys.* **2002**, *283*, 341.
- [30] A. Müller, F. Talbot, S. Leutwyler, *J. Am. Chem. Soc.* **2002**, *124*, 14486.
- [31] M. Meuwly, A. Müller, S. Leutwyler, *Phys. Chem. Chem. Phys.* **2003**, *5*, 2663.
- [32] A. Müller, M. Losada, S. Leutwyler, *J. Phys. Chem. A* **2004**, *108*, 157.
- [33] A. Müller, S. Leutwyler, *J. Phys. Chem. A* **2004**, *108*, 6156.
- [34] J.A. Frey, A. Müller, H.-M. Frey, S. Leutwyler, *J. Chem. Phys.* **2004**, *121*, 8237.
- [35] A. Müller, J.A. Frey, S. Leutwyler, *J. Phys. Chem. A* **2005**, *109*, in press.
- [36] B.B. Brady, L.A. Peteanu, D.H. Levy, *Chem. Phys. Lett.* **1988**, *147*, 538.
- [37] D. Onidas, D. Markovitsi, S. Marguet, A. Sharonov, T. Gustavsson, *J. Phys. Chem. B* **2002**, *106*, 11367.
- [38] T. Gustavsson, A. Sharonov, D. Markovitsi, *Chem. Phys. Lett.* **2002**, *351*, 195.
- [39] A. Held, D.W. Pratt, *J. Am. Chem. Soc.* **1990**, *112*, 8629.
- [40] A. Held, D.W. Pratt, *J. Chem. Phys.* **1992**, *96*, 4869.
- [41] T.R. Cech, S.H. Damberger, R.R. Gutell, *Nat. Struct. Biol.* **1994**, *1*, 273.
- [42] M. Grüne, J.P. Fürste, S. Klussmann, V.A. Erdmann, L.R. Brown, *Nucl. Acids Res.* **1996**, *24*, 2592.
- [43] J. Spöner, P. Hobza, *J. Phys. Chem. A* **2000**, *104*, 4592.
- [44] S.F. Boys, F. Bernardi, *Mol. Phys.* **1970**, *19*, 553.
- [45] W. Klopper, *J. Chem. Phys.* **1995**, *102*, 6168.
- [46] JAGUAR 5.0, Schrödinger, L.L.C., Portland, Oregon (1991–2003).
- [47] Gaussian 03, Rev. A.1, M.J. Frisch, G.W. Trucks, H.B. Schlegel *et al.*, Gaussian Inc., Pittsburgh, **2003**.
- [48] Vargas *et al.*[49] report an MP2/aug-cc-pVXZ CBS limit binding energy  $D_{CBS}^{\infty} = -14.35$  kcal/mol, about 3% smaller than that obtained here. The difference is due to (1) an error in their BSSE calculation, (2) the combination of fully correlated MP2 with aug-cc-pVXZ basis sets, which is inappropriate [53].
- [49] R. Vargas, J. Garza, R.A. Friesner, H. Stern, B.P. Hay, D.A. Dixon, *J. Phys. Chem. A* **2001**, *105*, 4963.
- [50] A.J. Cohen, N.C. Handy, *Chem. Phys. Lett.* **2000**, *316*, 160.
- [51] D.A. McQuarrie. *Statistical Mechanics*. Harper Collins, **1976**.
- [52] T.v. Mourik, R.J. Gdanitz, *J. Chem. Phys.* **2002**, *116*, 9620.
- [53] R.A. Kendall, T.H. Dunning, R.J. Harrison, *J. Chem. Phys.* **1992**, *96*, 6796.